

# Assessing Enzyme Immobilization on Reverse Asymmetric Membranes and Biocatalytic Reactor Performance

**Amirah Syakirah Zahirulain**

Universiti Teknologi MARA

**Fauziah Marpani** (✉ [fauziah176@uitm.edu.my](mailto:fauziah176@uitm.edu.my))

Universiti Teknologi MARA <https://orcid.org/0000-0002-0015-2421>

**Syazana Mohamad Pauzi**

Universiti Teknologi MARA

**'Azzah Nazihah Che Abd Rahim**

Universiti Teknologi MARA

**Hang Thi Thuy Cao**

Nha Trang Institute of Technology Research and Application

**Nur Hashimah Alias**

Universiti Teknologi MARA

**Nur Hidayati Othman**

Universiti Teknologi MARA

---

## Research Article

**Keywords:** Enzyme membrane reactor, Enzyme immobilization, Membrane fouling, Ultrafiltration, Biocatalytic productivity, Concentration polarization

**Posted Date:** November 8th, 2021

**DOI:** <https://doi.org/10.21203/rs.3.rs-931423/v1>

**License:** © ⓘ This work is licensed under a Creative Commons Attribution 4.0 International License.

[Read Full License](#)

---

1 **Assessing Enzyme Immobilization on Reverse Asymmetric Membranes and Biocatalytic**  
2 **Reactor Performance**

3 Amirah Syakirah Zahirulain<sup>a</sup>, \*Fauziah Marpani<sup>a</sup>, Syazana Mohamad Pauzi<sup>a</sup>, ‘Azzah Nazihah Che  
4 Abd Rahim<sup>a</sup>, Hang Thi Thuy Cao<sup>b</sup>, Nur Hashimah Alias<sup>a</sup> and Nur Hidayati Othman<sup>a</sup>

5 <sup>a</sup>School of Chemical Engineering, College of Engineering, Universiti Teknologi MARA, 40450 Shah  
6 Alam, Selangor Darul Ehsan, Malaysia

7 <sup>b</sup>NhaTrang Institute of Technology Research and Application, Vietnam Academy of Science and  
8 Technology, 02 Hung Vuong Street, Nhatrang 650000, Vietnam

9 \*Corresponding author email: [fauziah176@uitm.edu.my](mailto:fauziah176@uitm.edu.my)

10 Phone: +603 5543 6510 Fax: +603 5543 6300

11

12 **Acknowledgements:**

13 The study was funded by the Ministry of Higher Education Malaysia under the Fundamental Research  
14 Grants number FRGS/1/2019/TK02/UITM/03/5.

15

16

17

18

19

20

21

22

23 **Abstract**

24 Integration of membrane filtration and biocatalysis has appealing benefits in terms of simultaneous  
25 substrate conversion and product separation in one reactor. Nevertheless, the interaction between  
26 enzymes and membrane is complex and the mechanism of enzyme docking on membrane is similar to  
27 membrane fouling. In this study, focus is given on the assessment of enzyme immobilization mechanism  
28 on reverse asymmetric polymer membrane based on the permeate flux data during the procedure.  
29 Evaluation of membrane performance in terms of its permeability, fouling mechanisms, enzyme  
30 loading, enzyme reusability and biocatalytic productivity were also conducted. Alcohol Dehydrogenase  
31 (EC 1.1.1.1), able to catalyze formaldehyde to methanol with subsequent oxidation of NADH to NAD  
32 was selected as the model enzyme. Two commercial, asymmetric, flat sheet polymer membranes (PES  
33 and PVDF) were immobilized with the enzyme in the reverse mode. Combination of concentration  
34 polarization phenomenon and pressure driven filtration successfully immobilized almost 100% of the  
35 enzymes in the feed solutions. The biocatalytic membrane reactor recorded more than 90% conversion,  
36 stable permeate flux with no enzyme leaching even after 5 cycles. The technique showing promising  
37 results to be expanded to continuous membrane separation setup for repeated use of enzymes.

38

39

40

41

42

43

44

45 Keywords: Enzyme membrane reactor, Enzyme immobilization, Membrane fouling, Ultrafiltration,  
46 Biocatalytic productivity, Concentration polarization

## 47 **1. Introduction**

48 Enzyme is a useful biocatalyst that widely use in the industry due its green technology (Wohlgemuth  
49 2010). Enzyme catalyst can increase the rate of reaction up to  $10^{20}$  compared to traditional chemical  
50 catalyst that only increase  $10^2$  to  $10^4$  (Campbell and Farrel 2015). Furthermore, enzyme is more  
51 preferable because it have selectivity to produce higher preferred product compared to chemical  
52 catalyst (Zhang and Xing 2011). Even though enzyme can provide better greener sustainability and very  
53 helpful in the industry, the drawback of the enzyme is it is expensive and it is hard to remove from the  
54 reaction medium (Donato et al. 2014). Therefore, it need special requirement to use it such as  
55 reusability and immobilization to increase the efficiency of enzyme performance and commercialization  
56 potential (Luo et al. 2013).

57 Meanwhile, membrane is a material that consist of semi permeable polymeric material that use for  
58 separation of particle from the fluid. The particle that can pass through is based on different pore size  
59 and the construction of the membrane such as ultrafiltration, microfiltration and nanofiltration  
60 (Schaschke 2014). Ultrafiltration membrane is widely use in industry in drinking water and wastewater  
61 treatment process under filtration system (Gao et al. 2016). Recent researches show that membrane  
62 work together with enzyme to become biocatalytic membrane (Luo et al. 2020).

63 Enzymatic membrane reactor (EMR) is one type of membrane technology that integrate the membrane  
64 filtration and biocatalysis in one system which the enzyme will immobilize on the membrane  
65 (membrane work as support for enzyme). EMR widely use in wastewater treatment and it is a eco-  
66 friendly technology because it use mild condition in term of pH, temperature and pressure (Zdarta et al.  
67 2019). It help enzyme to enhance the biocatalysis and remove the product after achieve reaction (Zdarta  
68 et al. 2019).

69 There are a few techniques in immobilizing the enzyme such as adsorption, entrapment, cross-linking,  
70 covalent bonding and affinity. Every technique of immobilizing the enzyme has its advantages and  
71 disadvantages (Cao 2011; Zhang and Xing 2011; Datta et al. 2013; Nguyen and Kim 2017; Cen et al.  
72 2019). Immobilizing the enzyme can be the solution to control the enzyme drawbacks of purchasing

73 cost and hard to remove from reaction (Cao 2011). Immobilizing the enzyme have more advantages  
74 compared to the free enzyme which it is more stable compared to the free enzyme (Konovalova et al.  
75 2016)(Vitola et al. 2016). It also has more enzyme loading and enzymatic activities compared to the  
76 free enzyme (Xu et al. 2017). Plus, immobilizing enzyme on the membrane also can help enzyme  
77 improves its reusability. Enzyme reusability is useful in industry because it will be reducing the cost of  
78 enzyme purchasing (Amaly et al., 2018). Certain enzymes can withstand its activity in certain reaction  
79 cycle. For example, the lipase's enzyme activities decrease slowly and 69% of its activities remain after  
80 10 cycles on nanofibrous membrane (J. Zhu & Sun, 2012).

81 However, enzyme docking on the membrane causing membrane fouling therefore reducing the  
82 membrane performance in term of separation efficiency and permeate flux (Zdarta et al. 2019). There  
83 are a few types of membrane fouling such as pore blocking, physical adsorption, gel or cake formation  
84 or biofouling (Luo et al. 2014b) (Luo et al. 2014a). Even though fouling reducing the membrane  
85 performance, it also a strategy to use membrane weakness to fully utilize the enzyme by improvise the  
86 membrane function (work as enzyme support) since the enzyme immobilization and membrane fouling  
87 have similarities (Luo et al. 2013).

88 Since the enzyme can be immobilized on the membrane, we hypothesized that the different type of  
89 membranes (on reverse mode) will give different degree of membrane and biocatalytic performance  
90 and reusability of enzyme. Reverse mode is when support layer of the membrane facing feed in dead  
91 end set up. In this study, the assessment is conducted to investigate the enzyme immobilization  
92 mechanism on reverse asymmetric polymer membrane. The set-up of the enzymatic membrane reactor  
93 and the enzyme used in the research will be controlled so the membrane performance, biocatalytic  
94 performance and enzyme reusability can be evaluate. Enzyme immobilization of ADH is conducted on  
95 the propylene support layer of 2 commercial polymer membranes (PES and PVDF) for the development  
96 of enzymatic membrane reactor. Mechanism of enzyme adsorption on the membrane fibrous structure  
97 is discussed. The performance of the enzymatic membrane reactor is evaluated in terms of the  
98 membrane permeability, membrane fouling and enzyme reusability.

99

100 **2. Methodology**

101

102 *2.1 Chemicals and membranes*

103 Alcohol dehydrogenase from *Saccharomyces cerevisiae* (ADH, EC 1.1.1.1),  $\beta$ -Nicotinamide adenine  
104 dinucleotide, reduced disodium salt hydrate (NADH), formaldehyde (37% w/w), potassium phosphate  
105 monobasic ( $\text{KH}_2\text{PO}_4$ ), dipotassium hydrogen phosphate ( $\text{K}_2\text{HPO}_4$ ) and ethanol (98% v/v) were  
106 purchased from Sigma Aldrich (St. Louis, MO, USA). The molecular weights of ADH, NADH, and  
107 formaldehyde are 141000, 700, and 30 Da, respectively.  $\text{KH}_2\text{PO}_4$  and  $\text{K}_2\text{HPO}_4$  are diluted together in  
108 ultrapure water to make 0.1M phosphate buffer solution of pH 7. All enzyme and substrate solutions  
109 are prepared by using this buffer solution unless otherwise stated. Commercial membranes used in this  
110 experiment are ultrafiltration membranes from Synder Filtration (Vacaville, California, USA). The  
111 detail properties of both membranes are summarized in Table 1.

112 Table 1: Properties of commercial flat sheet polymer membranes.

Characteristics	Information	
Membrane	PES	PVDF
Manufacturer	Synder	Synder
pH range operation	1-11	1-11
Molecular weight cut off (kDa)	50	30
Membrane surface area ( $\text{cm}^2$ )	13.4	13.4
Skin material	Poly(ether)sulfone (PES)	Polyvinylidene fluoride (PVDF)
Support material	Polypropylene	Polypropylene
Isoelectric point (IEP)	pH 4.9 <sup>a</sup>	pH3.5 <sup>b</sup>
Contact angle		
Thickness (mm) <sup><math>\gamma</math></sup>	0.16	0.17
Permeability ( $\text{L}/\text{m}^2 \cdot \text{h} \cdot \text{bar}$ ) <sup><math>\gamma</math></sup>	72.3	100.0

113 <sup>a</sup>(Zhao et al. 2003)

114 <sup>b</sup>(Schulze et al. 2016)

115  <sup>$\gamma$</sup> Own measurement

116

117

118

119

120 2.2 *Experiment procedures*

121 2.2.1 *Cell setup*

122 The membrane was cut and fixed, reverse mode in a 50 ml dead-end Amicon stirred cell (Milipore,  
123 USA). Reverse mode is when the support layer is facing the feed and the skin layer is supported by  
124 another polypropylene layer. The membrane was soaked in a mixture of ethanol (50% v/v) for 10  
125 minutes following the manufacturer's instruction. The cleaned membrane will be filtered with ultrapure  
126 water at a pressure of 3 bar and 100 rpm in stirred cell in normal orientation (skin layer facing feed).  
127 After compression, 50 ml of ultrapure water is introduced in the stirred cell and the membrane is set up  
128 in reverse mode to determine the permeability with applied pressure of 1 bar and 100 rpm of stirring.

129

130 2.2.2 *Enzyme immobilization*

131 The feed for immobilize reaction contained 0.1 g/L of ADH in a 100 mM phosphate buffer solution pH  
132 7. The condition of the stirred cell is in 1 bar pressure and 100 rpm. The time taken for 4 ml aliquot of  
133 permeate was recorded and the sample was collected. The samples are then assayed with Bradford  
134 Reagent to determine ADH rejection (immobilization) by the membrane using UV-VIS  
135 spectrophotometer (Cary60, Agilent, USA) at a wavelength of 340 nm.

136

137 2.2.3 *Biocatalysis*

138 The reaction feed contained 30 ml of 100  $\mu$ M of formaldehyde and 100  $\mu$ M of NADH. The substrates  
139 were diluted in 100 mM phosphate buffer solution pH 7. A pressure of 2 bar and 100 rpm stirring was  
140 applied. 4 ml aliquot of permeate was collected and the time taken was recorded. The sample was then  
141 analysed for the remaining NADH available with UV-VIS spectrophotometer (Cary60, Agilent, USA)  
142 at a wavelength of 340 nm. The sample was then assayed with Bradford reagent to analyse for any  
143 enzyme leakage in the permeate. The feed was re-introduced for 5 cycles to observe the enzymatic  
144 reusability and biocatalytic productivity.

145 2.2.4 Contact angle measurement

146 The surface hydrophilicity of PES & PVDF membrane is measured by using contact angle goniometer  
147 instrument (AST/VCA-3000s). The angle of the water and both membranes is measured. The  
148 measurement is taken 3 times for both membranes and the results are compared.

149

150 2.3 Determination of various parameters

151 The percentage of enzyme loading is the calculation to determine the efficiency of enzyme  
152 immobilizing on/in the membrane. The formula of the percentage of enzyme loading is:

153 
$$\text{Enzyme Loading (\%)} = \frac{m_i}{m_f} \times 100 \quad (1)$$

154 where  $m_i$  is the amount of the enzyme that immobilized and  $m_f$  is the amount of enzyme in the feed  
155 solution.

156 Flux recovery ratio (FRR) is a calculation to identify the type of fouling resistance that forms on the  
157 membrane surface by taking the flux of the permeate. The formula for FRR is:

158 
$$\text{FRR (\%)} = \left( \frac{J_{w2}}{J_{w1}} \right) \times 100 \quad (2)$$

159 Total fouling ratio ( $R_t$ ), reversible resistance ( $R_r$ ) and irreversible resistance ( $R_{ir}$ ) are calculated as  
160 follow:

161 
$$R_t (\%) = \left( 1 - \frac{J_p}{J_{w1}} \right) \quad (3)$$

162 
$$R_r (\%) = \left( \frac{J_{w2} - J_p}{J_{w1}} \right) \quad (4)$$

163 
$$R_{ir} (\%) = \left( \frac{J_{w1} - J_{w2}}{J_{w1}} \right) \quad (5)$$

164 Where  $J_p$  = permeate flux;  $J_{w1}$  = initial pure water flux and  $J_{w2}$  = final pure water flux

165 The conversion rate of reaction is calculated to determine the conversion of NADH by the enzyme.

166 The formula of the conversion rate is:

167 
$$\text{Conversion rate (\%)} = \frac{C_f - C_p}{C_f} \times 100 \quad (6)$$

168 where  $C_f$  is the concentration of NADH in the feed solution and  $C_p$  is the concentration of NADH in  
169 permeate solution.

170 Biocatalytic productivity is a calculation to calculate the efficiency of the enzyme converting substrate  
171 to product. The formula for the biocatalytic productivity is:

172 
$$\text{Biocatalytic productivity} = \frac{m_p}{m_e} \quad (7)$$

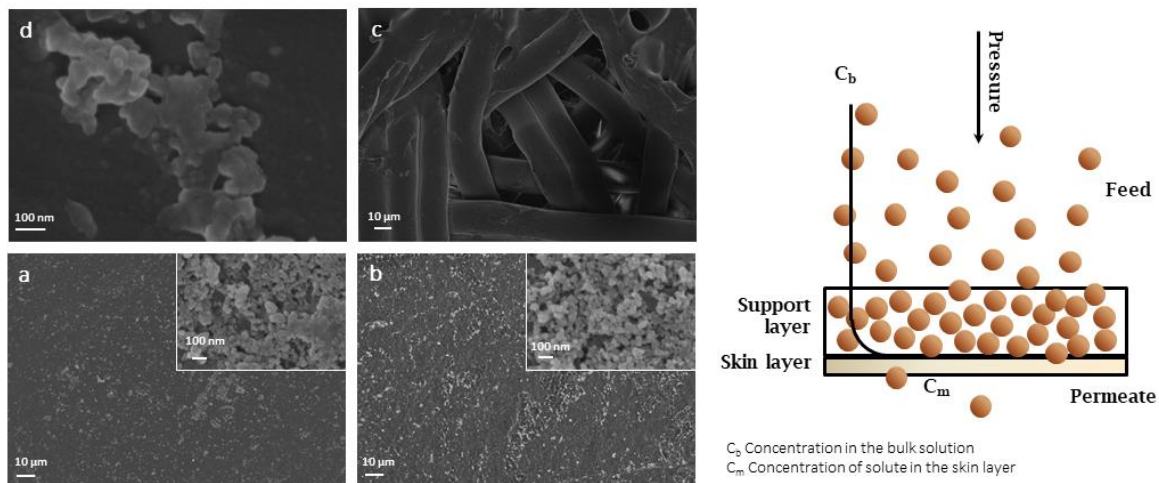
173 where  $m_p$  is the mass of the production and  $m_e$  is the mass of the enzyme.

174

### 175 **3. Results and Discussion**

#### 176 *3.1 Biocatalytic membrane reactor configuration and mechanism of enzyme immobilization*

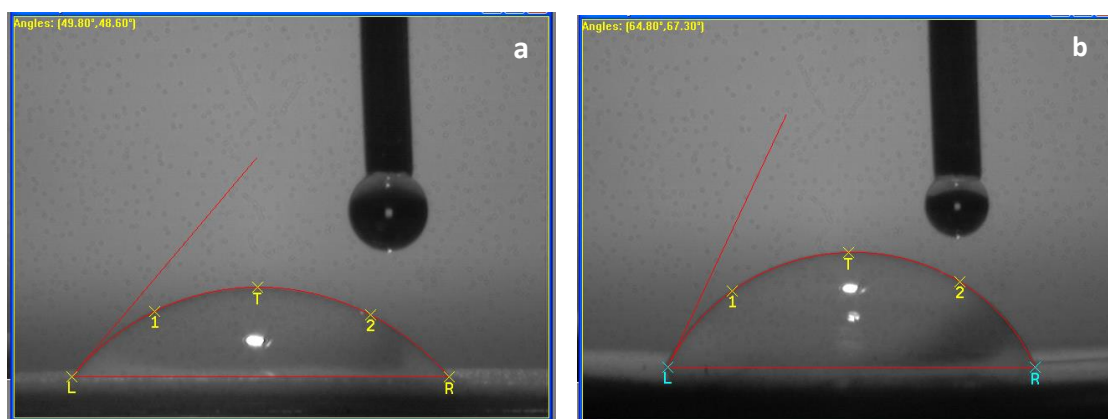
177 Two types of commercial membranes, PES and PVDF were used in this work. The polymer membranes  
178 are asymmetric, characterized by its anisotropic structure, comprised of two main layers with different  
179 properties in morphology and permeability. The active layer with the MWCO specification is denoted  
180 as the skin layer (Figure 1a&b), whereas the fibrous structure (Figure 1c) is the support layer.  
181 Experiment is designed to immobilize ADH in the support layer of the membrane. Utilising reverse  
182 asymmetric membrane will cause concentration polarization and subsequently leads to membrane  
183 fouling (Guerra et al. 1997). This is advantageous in ensuring maximum enzymes can be immobilized  
184 and preventing enzyme from leaching out because of the dense feature of the skin layer (Figure 1)  
185 (Marpani et al. 2015). As shown in Table 2, both membranes successfully immobilized almost 100%  
186 of enzymes in the feed solution. There was no leaching out of enzymes observed throughout the  
187 experiment.



188

189 Figure 1: Illustration of concentration profile for feed stream at the surface of the support layer. Inserted  
 190 SEM images of the polymer membrane, (a) PES skin layer; (b) PVDF skin layer; (c) the membrane  
 191 support layer; (d) closed-up image of the membrane support layer.

192



193

194 Figure 2: Contact angle measurement for a) PVDF and b) PES membranes.

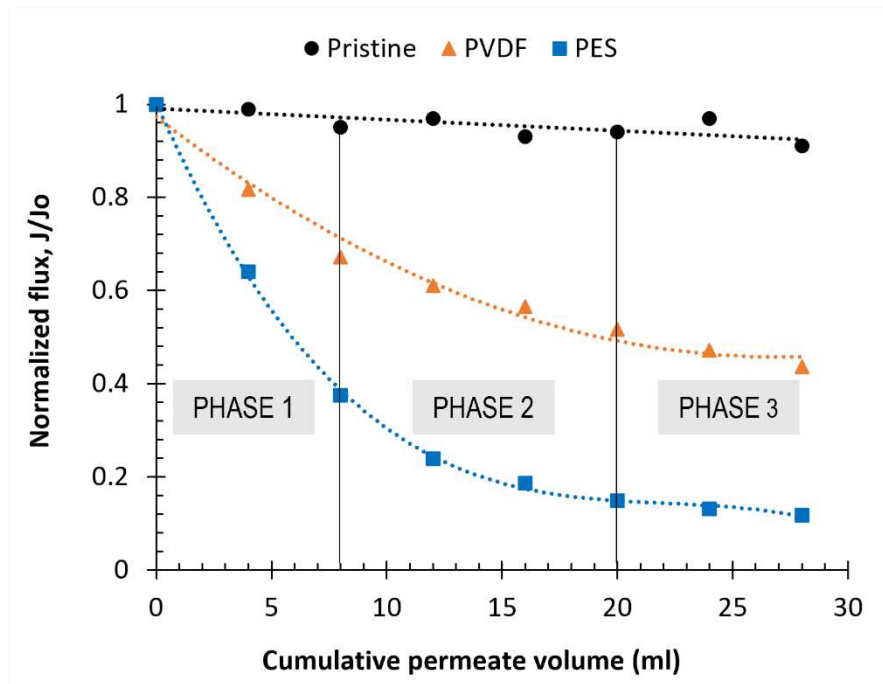
195

196 Table 2: Enzyme loading on PES and PVDF membrane.

Membrane	Amount of Enzyme (mg)					Percent Loading (%)
	Feed	Permeate	Retentate	Washing	Loading	
PES	3	0.0028	0.0174	0.0058	2.9741	99.14
PVDF	3	0.0007	0.0780	0.0455	2.9667	98.89

197 During the filtration of ADH, a high local concentration of enzyme will arise near the support layer-  
198 solution interface, due to a balance between the convective drag force towards and through the  
199 membrane and back transport away from the membrane (Figure 1). This phenomenon is called  
200 concentration polarization (CP). CP will result in flux decline due to the increment of the osmotic  
201 pressure near the surface of the membrane. Hence, the effectiveness of pressure-driven filtration is  
202 reduced. Figure 3 shows the flux profile during enzyme immobilization which shows 3 phases of flux  
203 decline related to enzyme deposition mechanism in/on the membrane. The initial phase (Phase 1)  
204 includes macromolecular sorption and particle deposition. Fresh membrane is exposed to the ADH and  
205 adsorb onto the polypropylene fibrous strand (Figure 1c&d). Part of the ADH may aggregate because  
206 of electrostatic forces (from ionizable chemical species in the buffer) and build up in between the  
207 support and skin layer interface. These aggregates then served as nucleation sites for the continued  
208 deposition of other enzymes. As can be observed in Figure 1a&b, the skin layer is dense, and the pores  
209 are too small for the ADH to pass through. In Phase 2, the first sublayer developed into multi-sublayers  
210 and increase the osmotic pressure which in turn compresses the sublayers. Permeate flux decline is more  
211 prominent at the end of this phase. In the final phase (Phase 3), the ADH in the sublayer rearrange  
212 themselves and finally stabilized. All enzymes are supposed to be immobilized at this stage.

213



214

215

Figure 3: Flux profile during enzyme immobilization showing 5 different phases.

216

Another mechanism responsible for the docking of ADH on the surface of the membrane is charge

217

interaction. Membrane charge is significant separating factor for ultrafiltration, nanofiltration and

218

reverse osmosis membranes (Oatley-Radcliffe et al. 2017) driving the attachment of ADH enzymes in

219

the membrane support layer. Membrane is composed of polymer repeating units (Scheme 1). PES for

220

example, composed of the  $\text{SO}_3\text{H}$  functional group, a strong acidic group, which dissociates over a very

221

wide pH range (Oatley-Radcliffe et al. 2017). Membrane develop charge by the adsorption of charged

222

elements from dissociation of functional groups of the membrane (polyelectrolytes), ions in the buffer

223

solution and macromolecules (ADH and respective substrates). These charged species physically adsorb

224

to the surface of the membrane through van de Waals forces (Childress and Elimelech 2000). The buffer

225

solution used in this experiment is at pH 7. The isoelectric point (pI) of ADH, and propylene support

226

layer, PES and PVDF skin layer are 5.4-5.8 (Luo et al. 2014a), 3.3 (Smole et al. 2009), 4.9 (Zhao et al.

227

2003) and 3.5 (Schulze et al. 2016) respectively. The ADH and the membrane elements will be

228

negatively charged and should cause repulsion between the membrane and the charged solute of feed

229

solution. Nevertheless, the membrane skin layers are both hydrophilic. Hydrophilic surfaces reduce

230 electrostatic charge accumulation (Omastova 2016) and combined with the pressure driven dead-end  
231 filtration aid in the docking of enzyme in/on the membrane.

232 The permeate flux of PES and PVDF membranes decreases as the cumulative volume of permeate  
233 increasing. This is because of the increasing of concentration polarization that happens on the surface  
234 of the membrane. The concentration polarization is increase when the fouling on/in the membrane  
235 increase (Giacobbo et al. 2018). In our study, this is desirable because it indicates that the enzyme is  
236 successfully adsorbed and fouled the membrane.

237

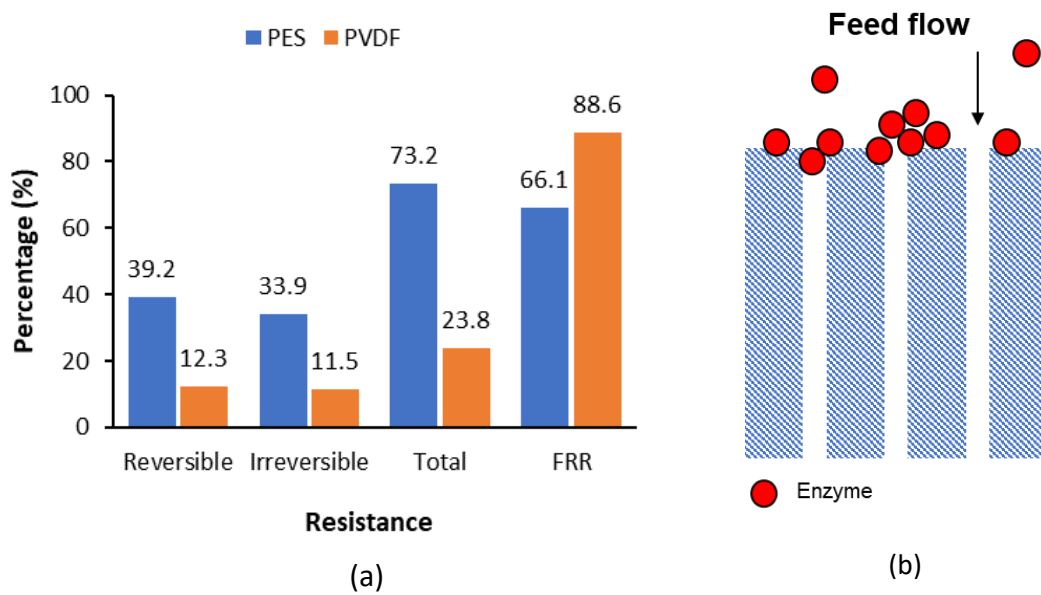
### 238 3.2 Evaluation of membrane fouling

239 As described in the previous section, the governing mechanism of membrane fouling due to enzyme  
240 immobilization procedure in this study is macromolecular adsorption. Two models were applied to  
241 evaluate membrane fouling in this study, namely the flux recovery ratio (FRR) and Hermia's model.  
242 Hermia's model is used because it is the most comprehensive prediction models presenting membrane  
243 fouling scenario which includes complete blocking, standard blocking, intermediate blocking, or cake  
244 layer (Chang et al. 2011; Wang et al. 2012). Furthermore, it suitable to use for the dead-end membrane  
245 separation (Ismail et al. 2021). FRR measures antifouling properties of the membrane. Generally, a  
246 lower FRR indicates serious membrane fouling. PES obtained higher percentage FRR with 88.6%,  
247 compared to PVDF with 66.1% (Figure 4). This could indicate that the fouling in PES is more critical  
248 than PVDF, even though both membranes load almost the same amount of enzymes (Table 2).

249 As shown in Figure 4, PES and PVDF membranes have a higher percentage ratio of reversible resistance  
250 with 39.24% and 12.25% respectively, compared to the irreversible resistance with 33.92% and 11.45%  
251 respectively. Reversible resistance is where the fouling agents (ADH) that are loosely attached to the  
252 membrane and possible to be desorbed to the bulk solution. On the other hand, irreversible fouling  
253 indicates that the fouling agents are tightly bound to the membrane and no possibility of desorption to  
254 the bulk solution. A lower total resistance ratio ( $R_t$ ) will cause a higher FRR resulting in a lower total  
255 flux loss as compared to the pristine membrane.

256 From the regression data summarized in Table 3, intermediate fouling (Figure 4b) is predicted using  
 257 Hermia’s model for both membranes suggesting that each foulant has a probability to either deposit on  
 258 an unobstructed area of the membrane or deposit onto a previously deposited foulant particle (Kirschner  
 259 et al. 2019). This is in line with the estimation of total resistance where it was found that reversible  
 260 fouling is higher than irreversible fouling in PES and PVDF membrane.

261



262

263 Figure 4: (a) Membrane resistance and flux recovery ratio (FRR) of PES and PVDF membranes and (b)  
 264 Illustration of intermediate fouling by Hermia’s model.

265

266 Table 3: Regression data to determine membrane fouling mechanism according to Hermia’s model.

Membrane	Membrane Fouling Mechanism			
	Complete	Standard	Intermediate	Cake
PES	0.9597	0.9901	1.0000	0.9685
PVDF	0.9974	0.9994	1.0000	0.9974

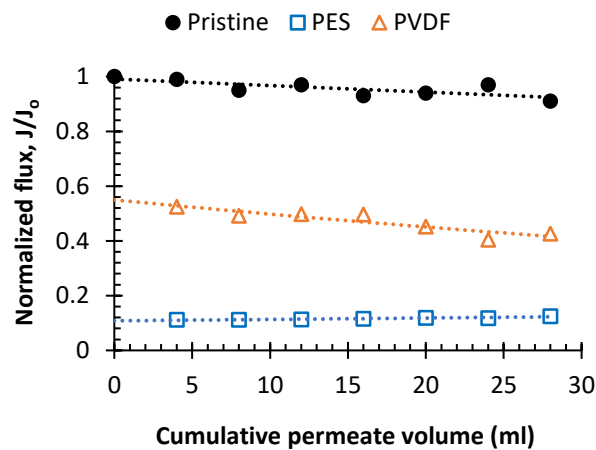
267

268

269

270 3.3 Enzymatic membrane reactor performance

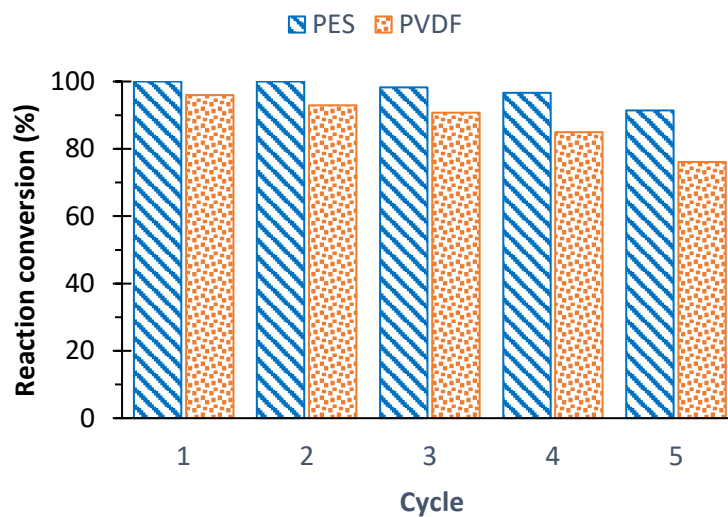
271 The permeate flux of PVDF membrane is higher compared to the permeate flux of PES membrane  
272 during reaction (Figure 5). Both permeate flux profiles are stable at and have the same value as permeate  
273 flux at the end of Phase 3 during enzyme immobilization procedure (Figure 2). Even though the MWCO  
274 of PES is larger than PVDF (Table 1), the permeate flux profiles are contradicted due to the enzyme  
275 immobilization mechanism as discussed in section 3.1.



276

277

Figure 5: Flux profile during the reaction.



278

279

Figure 6: Percentage conversion of formaldehyde to methanol for 5 cycles.

280

281 Figure 6 shows the percentage reaction conversion of formaldehyde to methanol for 5 cycles. The  
282 average conversion for PES membrane is higher than PVDF membrane. ADH enzyme on the PES  
283 membrane can retain its activity above 80% within five cycles while the ADH enzyme on the PVDF  
284 membrane can retain its enzyme activity above 50%. In previous research, ADH retain its activity at  
285 20.1% and 79.6% of its original activity on MNP-ADH and MGO-ADH membrane respectively (Liu  
286 et al. 2015). Despite the amount of enzyme immobilized is almost the same for both membranes (Table  
287 2), the productivity is not corresponded to it. Biocatalytic productivity for PES and PVDF membrane  
288 is 5.2 and 4.7 mg methanol/mg ADH respectively. This is very much related to the arrangement of  
289 enzymes in/on the membrane due to the enzyme-enzyme and enzyme-membrane interactions. Protein  
290 molecules are surrounded by a hydration shell in solution (Chen and Sun 2003). In the presence of salt  
291 (buffer) and ionizable chemical species, the hydration shell will be stripped off from the protein  
292 molecule due to the hydration effect of the salt molecules of the protein environment (Lin et al. 2000).  
293 This will result with an exposed area of hydrophobic zones of the enzymes making the hydrophobic  
294 interactions between the ADH and the adsorbent surface (polypropylene) become stronger. The  
295 hydrophobic interactions will induce conformational changes of the enzyme structure thus altering its  
296 activity. It is also believed that high permeate flux during reaction by a more hydrophilic PVDF  
297 membrane, thus some of the substrate not in contact with enzyme while passing through the membrane.  
298 Slower permeate of PES during immobilization would distribute enzyme evenly on the polypropylene  
299 fibre strands and skin-support interface, hence slower permeate flux during reaction ensuring optimum  
300 contact time with substrate.

301

#### 302 **4. Conclusion**

303 The fibrous structure of asymmetric membrane support layer has the potential to be exploited as the  
304 enzyme immobilization matrix. Almost 100% of enzymes in the feed were successfully immobilized  
305 following adsorption mechanism and charge interaction. A combination of concentration polarization  
306 effect which is critical in dead end filtration method and convective transport, drive the mass transfer  
307 of the enzymes and further, aided in the docking. There are three phases of permeate flux decline which

308 are strongly related to the process of enzyme adsorption mechanism in the membrane, following this  
309 pattern: molecular sorption and particle deposition – development of multi-sublayers – sublayers  
310 rearrangement and stabilization. Ionizable chemical components and membrane surface, van der Waals  
311 force, isoelectric point are consolidated factors, responsible for the membrane charges interaction which  
312 further aid in the enzyme's entrapment. Membrane fouling is described via Hermia's model and flux  
313 recovery ratio. Both models conclude that intermediate fouling dominates. Reversible fouling is higher  
314 than irreversible for both membranes, but the intensity of irreversible fouling is more prominent in PES,  
315 indicating fouling is severe in PES. The system showed stable, high enzyme conversion of more than  
316 80% of formaldehyde to methanol in five cycles. This promotes a good biocatalytic productivity data  
317 for the enzymes proving that enzyme immobilization in the reverse asymmetric membrane feasible to  
318 be applied in other biocatalytic reactions.

319

## 320 **Declarations**

321 *Ethics approval and consent to participate:* Not applicable

322 *Consent for publication:* Not Applicable

323 *Availability of data and materials:* Not applicable

324 *Competing interests:* The authors declare that they have no competing interests.

325 *Funding:* The study which includes material and chemicals procurement, and experimental analysis  
326 was funded by the Ministry of Higher Education Malaysia under the Fundamental Research Grants  
327 number FRGS/1/2019/TK02/UITM/03/5. Amirah Syakirah Zahirulain emolument is funded under the  
328 graduate research assistant vote 11000 of the grant.

329 *Authors' contributions:* ASZ conduct the experiments, collecting data for analysis writing the  
330 manuscript. FM secured the grants, supervising ASZ, research framework and manuscript writing. SMP  
331 and ANR partly writing the manuscript Section 3.2. HC responsible on polishing the introduction  
332 section. NHO and NHA advise on the structure of the manuscript and proof reading.

333 *Acknowledgements:* The study was funded by the Ministry of Higher Education Malaysia under  
334 Fundamental Research Grants number FRGS/1/2019/TK02/UITM/03/5.

335

## 336 **References**

337 Campbell MK, Farrel SO (2015) The behaviour of protein: enzyme. In: Biochemistry, 8th Editio.

338 Cengage Learning, Stamford, pp 133–155

339 Cao L (2011) Immobilized Enzymes, Second Edi. Elsevier B.V.

340 Cen YK, Liu YX, Xue YP, Zheng YG (2019) Immobilization of Enzymes in/on Membranes and their

341 Applications

342 Chang EE, Yang SY, Huang CP, et al (2011) Assessing the fouling mechanisms of high-pressure

343 nanofiltration membrane using the modified Hermia model and the resistance-in-series model.

344 Sep Purif Technol 79:329–336. <https://doi.org/10.1016/j.seppur.2011.03.017>

345 Chen J, Sun Y (2003) Modeling of the salt effects on hydrophobic adsorption equilibrium of protein. J

346 Chromatogr A 992:29–40. [https://doi.org/10.1016/S0021-9673\(03\)00277-2](https://doi.org/10.1016/S0021-9673(03)00277-2)

347 Childress AE, Elimelech M (2000) Relating nanofiltration membrane performance to membrane

348 charge (electrokinetic) characteristics. Environ Sci Technol 34:3710–3716.

349 <https://doi.org/10.1021/es0008620>

350 Datta S, Christena LR, Rajaram YRS (2013) Enzyme immobilization: an overview on techniques and

351 support materials. 3 Biotech 3:1–9. <https://doi.org/10.1007/s13205-012-0071-7>

352 Donato L, Algieri C, Rizzi A, Giorno L (2014) Kinetic study of tyrosinase immobilized on polymeric

353 membrane. J Memb Sci 454:346–350. <https://doi.org/10.1016/j.memsci.2013.12.029>

354 Gao F, Wang J, Zhang H, et al (2016) Effects of sodium hypochlorite on structural/surface

355 characteristics, filtration performance and fouling behaviors of PVDF membranes. J Memb Sci

356 519:22–31. <https://doi.org/10.1016/j.memsci.2016.07.024>

357 Giacobbo A, Bernardes AM, Rosa MJF, De Pinho MN (2018) Concentration polarization in  
358 ultrafiltration/nanofiltration for the recovery of polyphenols from winery wastewaters.  
359 Membranes (Basel) 8:. <https://doi.org/10.3390/membranes8030046>

360 Guerra A, Jonsson G, Rasmussen A, et al (1997) Low cross-flow velocity microfiltration of skim milk  
361 for removal of bacterial spores. *Int Dairy J* 7:849–861. [https://doi.org/10.1016/S0958-](https://doi.org/10.1016/S0958-6946(98)00009-0)  
362 [6946\(98\)00009-0](https://doi.org/10.1016/S0958-6946(98)00009-0)

363 Ismail FH, Marpani F, Othman NH, Nik Him NR (2021) Simultaneous separation and biocatalytic  
364 conversion of formaldehyde to methanol in enzymatic membrane reactor. *Chem Eng Commun*  
365 208:636–645

366 Konovalova V, Guzikevich K, Burban A, et al (2016) Enhanced starch hydrolysis using  $\alpha$ -amylase  
367 immobilized on cellulose ultrafiltration affinity membrane. *Carbohydr Polym* 152:710–717.  
368 <https://doi.org/10.1016/j.carbpol.2016.07.065>

369 Lin FY, Chen WY, Ruaan RC, Huang HM (2000) Microcalorimetric studies of interactions between  
370 protein and hydrophobic ligands in hydrophobic interaction chromatography: effects of ligand  
371 chain length, density, and the amount of bound protein. *Prog Biotechnol* 16:59–62.  
372 [https://doi.org/10.1016/S0921-0423\(00\)80013-1](https://doi.org/10.1016/S0921-0423(00)80013-1)

373 Liu L, Yu J, Chen X (2015) Enhanced stability and reusability of alcohol dehydrogenase covalently  
374 immobilized on magnetic graphene oxide nanocomposites. *J Nanosci Nanotechnol* 15:1213–  
375 1220. <https://doi.org/10.1166/jnn.2015.9024>

376 Luo J, Marpani F, Brites R, et al (2014a) Directing filtration to optimize enzyme immobilization in  
377 reactive membranes. *J Memb Sci* 459:1–11. <https://doi.org/10.1016/j.memsci.2014.01.065>

378 Luo J, Meyer AS, Jonsson G, Pinelo M (2013) Fouling-induced enzyme immobilization for  
379 membrane reactors. *Bioresour Technol* 147:260–268.  
380 <https://doi.org/10.1016/j.biortech.2013.08.019>

381 Luo J, Meyer AS, Jonsson G, Pinelo M (2014b) Enzyme immobilization by fouling in ultrafiltration

382 membranes: Impact of membrane configuration and type on flux behavior and biocatalytic  
383 conversion efficacy. *Biochem Eng J* 83:79–89. <https://doi.org/10.1016/j.bej.2013.12.007>

384 Luo J, Song S, Zhang H, et al (2020) Biocatalytic membrane: Go far beyond enzyme immobilization.  
385 *Eng. Life Sci.* 20:441–450

386 Marpani F, Luo J, Mateiu RV, et al (2015) In Situ Formation of a Biocatalytic Alginate Membrane by  
387 Enhanced Concentration Polarization. *ACS Appl Mater Interfaces* 7:17682–17691.  
388 <https://doi.org/https://doi.org/10.1021/acsami.5b05529>

389 Nguyen HH, Kim M (2017) An Overview of Techniques in Enzyme Immobilization. *Appl Sci*  
390 *Converg Technol* 26:157–163. <https://doi.org/10.5757/asct.2017.26.6.157>

391 Oatley-Radcliffe DL, Aljohani N, Williams PM, Hilal N (2017) Electrokinetic Phenomena for  
392 Membrane Charge. In: *Membrane Characterization*. Elsevier B.V., pp 405–422

393 Omastova M (2016) Effect of antistatic agents on some properties of compounded materials. In:  
394 *Handbook of Antistatics*. pp 149–182

395 Schaschke C (2014) *Dictionary of Chemical Engineering, First*. Oxford University Press, Oxford

396 Schulze A, Went M, Prager A (2016) Membrane functionalization with hyperbranched polymers.  
397 *Materials (Basel)* 9:. <https://doi.org/10.3390/ma9080706>

398 Smole MSS, Stakne K, Kleinschek KS, et al (2009) Electrokinetic properties of polypropylene-  
399 layered silicate nanocomposite fibers. *J Appl Polym Sci* 113:1276–1281.  
400 <https://doi.org/https://doi.org/10.1002/app.30083>

401 Vitola G, Mazzei R, Fontananova E, et al (2016) Polymeric biocatalytic membranes with immobilized  
402 thermostable phosphotriesterase. *J Memb Sci* 516:144–151.  
403 <https://doi.org/10.1016/j.memsci.2016.06.020>

404 Wang C, Li Q, Tang H, et al (2012) Membrane fouling mechanism in ultrafiltration of succinic acid  
405 fermentation broth. *Bioresour Technol* 116:366–371.

406 <https://doi.org/10.1016/j.biortech.2012.03.099>

407 Wohlgemuth R (2010) Biocatalysis-key to sustainable industrial chemistry. *Curr Opin Biotechnol*  
408 21:713–724. <https://doi.org/10.1016/j.copbio.2010.09.016>

409 Xu R, Cui J, Tang R, et al (2017) Removal of 2,4,6-trichlorophenol by laccase immobilized on nano-  
410 copper incorporated electrospun fibrous membrane-high efficiency, stability and reusability.  
411 *Chem Eng J* 326:647–655. <https://doi.org/10.1016/j.cej.2017.05.083>

412 Zdarta J, Meyer AS, Jesionowski T, Pinelo M (2019) Multi-faceted strategy based on enzyme  
413 immobilization with reactant adsorption and membrane technology for biocatalytic removal of  
414 pollutants: A critical review. *Biotechnol Adv* 37:107401.  
415 <https://doi.org/10.1016/j.biotechadv.2019.05.007>

416 Zhang C, Xing XH (2011) *Enzyme Bioreactors*, Second Edi. Elsevier B.V.

417 Zhao ZP, Wang Z, Wang SC (2003) Formation, charged characteristic and BSA adsorption behavior  
418 of carboxymethyl chitosan/PES composite MF membrane. *J Memb Sci* 217:151–158.  
419 [https://doi.org/10.1016/S0376-7388\(03\)00105-4](https://doi.org/10.1016/S0376-7388(03)00105-4)

420